doi:10.14311/ppt.2019.2.144

Plasma Physics and Technology **6**(2):144–147, 2019

RADIATIVE PROPERTIES AND NUMERICAL MODELING OF C_4F_7N-CO_2 THERMAL PLASMA

M. Gnybida[a,*], Ch. Rümpler[b], V.R.T. Narayanan[a]

[a] *Eaton European Innovation Center, Bořivojova 2380, 252 63 Roztoky, Czech Republic*

[b] *Eaton Industries GmbH, Hein-Moeller-Straße 7-11, 53115 Bonn, Germany*

[*] MykhailoGnybida@Eaton.com

Abstract. C_4F_7N and $C_4F_7N - CO_2$ mixtures are considered as alternatives to SF_6 for use in medium voltage gas insulated switchgear applications (GIS), due to the low global warming potential and good dielectric properties of C_4F_7N. Current work is focused on the calculation of radiative properties (absorption coefficients) of $C_4F_7N - CO_2$ thermal plasma and computational fluid dynamics (CFD) simulations of free burning $C_4F_7N - CO_2$ arcs that are stabilized by natural convection. Absorption coefficients of $C_4F_7N - CO_2$ plasma used in the CFD model are derived from spectral absorption coefficients by Planck averaging. An optimization procedure has been applied to find the optimal number of spectral bands as well as spectral band interval boundaries. Radiation and flow model results for $C_4F_7N - CO_2$ in comparison to SF_6 and air are provided and discussed.

Keywords: radiation, thermal plasma, gas insulated switchgear, SF_6 alternative.

1. Introduction

Sulphur hexafluoride (SF_6) is commonly used in gas insulated switchgear applications (GIS) for medium voltage and high voltage applications. In case of medium voltage (1000 V to 52 kV), SF_6 is usually used as an electric insulation medium that provides significantly enhanced dielectric strength compared to air as insulation medium, which can be utilized to shrink the GIS switchgear design compared to air insulated designs. Switching in SF_6 is performed in some medium voltage applications too, e.g. load break switches. In case of high voltage switchgear applications (above 52 kV), SF_6 provides excellent electric insulation as well as interruption capabilities, which are used in GIS but also in circuit breaker applications.

One important drawback of SF_6 is the 23 500 times larger global warming potential (GWP) compared to CO_2. Because of this very high GWP, many alternative gases have been considered in pursue of replacing SF_6 in medium and high voltage switchgear and circuit breaker applications. One promising alternative gas is C_4 perfluoro-nitrile C_4F_7N, which has a GWP of 2 200 and its dielectric strengths is 2 times higher than SF_6. Because of the high boiling point of C_4F_7N, which is -4.7 °C at atmospheric pressure, this SF_6 alternative needs to be diluted with some other gas to avoid liquefaction. Otherwise the lower operating temperature limit might not be sufficient.

In this contribution, the radiative properties of C_4F_7N are calculated and applied in CFD models of free burning arcs that are stabilized by natural convection. Besides radiative properties, transport, and thermodynamic properties are needed as well to setup a complete model. The calculation approach and results are introduced in a companion paper of this conference [1]. Results of the radiation properties calculation and the CFD model for $C_4F_7N - CO_2$ will be compared with those of air and SF_6.

2. Radiative properties

Radiation transport is a very important part of power balance of a thermal plasma. The simplest approach to model the effect of radiation is the net emission coefficient (NEC) [2], which describes the net radiation from an isothermal sphere or cylinder. Although the knowledge of the NEC allows to estimate the radiation losses in the hottest regions of the arc, it cannot predict the reabsorption of radiation in the colder arc fringes and the radiative flux impinging on surrounding surfaces.

More capable radiation transfer models are the P1 and the discrete-ordinates method (DOM) [3]. With these models the radiation spectrum can be divided into several gray bands to take into account the spectral variation of radiative transport. A constant Planck or Rosseland averaged absorption coefficient is derived from the spectral absorption coefficient for the particular band. Instead of resolving the whole spectrum, the radiation transfer is solved for a small number of bands only, which does reduce the computational effort dramatically while providing reasonable accuracy. In this paper, we calculate Planck mean absorption coefficient $k_{\mathrm{Planck},i}$ for each band i according to:

$$k_{\mathrm{Planck},i} = \frac{\int_{\nu_i}^{\nu_{i+1}} k_\nu B_\nu \mathrm{d}\nu}{\int_{\nu_i}^{\nu_{i+1}} B_\nu \mathrm{d}\nu}\,, \qquad (1)$$

where the lower and upper interval boundaries (band limits) are denoted by ν_i and ν_{i+1} respectively and B_ν represents the black body radiative intensity. We

renormalize the line contribution of the spectral absorption coefficients according to [4] with a characteristic plasma absorption length $H = 3 \cdot R_\mathrm{p}$, as suggested in [5]. The plasma radius R_p is defined as radius value where the temperature decreased to 50% of the core temperature.

To determine the necessary number of bands and location of the band limits in the spectral range, optimization and verification procedures as introduced in [5–7] are applied to a specific mixture of C_4F_7N and CO_2. In the optimization procedure two infinitely long cylindrical calculation domains are considered, one with 3 cm and the other one having a 10 cm radius. Both profiles are discretized using 30 points. The plasma inside these domains shall be represented by a fixed temperature profile along the radius, as shown in Fig. 1.

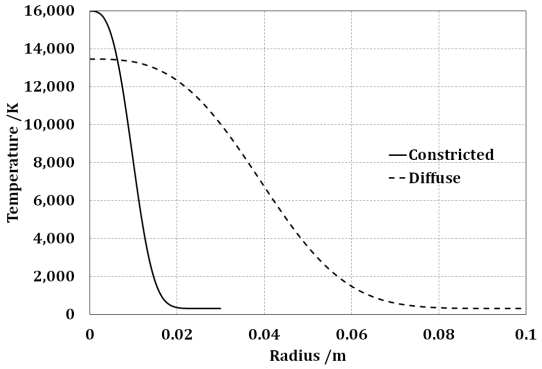

Figure 1. Assumed plasma temperature profiles.

The more constricted profile has a temperature maximum at 16 000 K while the diffuse profile is defined with a 13 460 K temperature maximum in the arc core. Each domain is evenly filled with a 90% CO_2 – 10% C_4F_7N gas mixture at atmospheric pressure (1 atm). For both profiles optimization runs were performed. The two temperature profiles are used to calculate the species compositions first, which are used as input for the calculation of the spectral absorption coefficients k_ν. The frequency range in the calculation covers 10^{12} Hz to 10^{16} Hz with a frequency step size of $2 \cdot 10^{10}$ Hz. An example of the calculated spectral absorption coefficient with line and continuum contributions for a 90% CO_2 – 10% C_4F_7N gas mixture at 10 000 K and 1 atm is shown in Fig. 2.

A relative error norm $\Delta F'_\nu$ is used to quantify the difference between the spectrally resolved and the band averaged solution of the radiation transfer equation [6]:

$$\Delta F'_\nu = \sqrt{\frac{\sum_i \left(\nabla \cdot F_{\mathrm{exact},i} - \nabla \cdot F_{\mathrm{mean},i}\right)^2}{\sum_i \left(\nabla \cdot F_{\mathrm{exact},i}\right)^2}} \,, \qquad (2)$$

where $\nabla \cdot F_{\mathrm{exact},i}$ represents the divergence of the radiative flux calculated in the spectral solution for each point i and $\nabla \cdot F_{\mathrm{mean},i}$ represents the divergence of radiative flux calculated using the line limited Planck mean absorption coefficients.

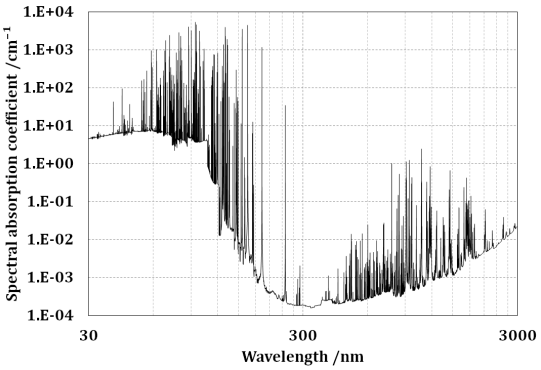

Figure 2. Spectral absorption coefficient for a 90% CO_2 and 10% C_4F_7N gas mixture at 10 000 K and 1 atm.

In this paper contributions from atomic and molecular radiation as well as continuum radiation are taken into account. Table 1 provides the list of species that are considered in the radiation calculations. The optimization procedure was performed for a different total number of bands (2 to 6) to analyze the dependency of accuracy of the band averaged model on the number of bands. An example of the optimization results for a 90% CO_2 – 10% C_4F_7N gas mixture and the diffuse temperature profile at 1 atm are shown in Fig. 3. As a major result the derived band boundaries for the different total number of bands are all located in UV region of the spectrum.

Atoms	N, O, C, F
Molecules	N_2, O_2, O_3, NO, C_2, C_3, C_4, CO, CN, CO_2, CN_2, C_2N, C_2N_2, C_2O, C_3O_2, F_2, CF, C_2F_2, C_2F_4, C_2F_6, CF_2, CF_3,CF_4, NF, NOF, NO_2F, FNO_3, NF_2, N_2F_2, F_2O, F_2O_2, NF_3, NOF_3, N_2F_4, NO_2, N_2O, COF_2
Electron and ions	e, N^+, N^{2+}, N^{3+}, N_2^+, O^+, O^{2+}, O^{3+}, O_2^+, NO^+, C^+, C^{2+}, C^{3+}, CO^+, CN^+, F^+, F^{2+}, F^{3+}

Table 1. List of species used in radiation calculations.

Corresponding error norm values according to Eq. 2 are provided in Fig. 4. The 2–band approximation results in an error of 12.98 % that is decreasing with increasing number of bands down to 2.55 % for 6 bands. A larger number of bands does improve the accuracy of the radiation model as expected, but the gain of accuracy using 6 bands rather than and 5 bands is only about 0.13 %. For this specific gas mixture and temperature profile, solving a 6–band model would not provide a much benefit over a 5–band model.

Although the 6–band approximation provides higher accuracy over the 3–band approximation, the 3–band approximation is used in subsequent arc modeling since a larger number of bands does increase the computational effort when solving radiation transfer. For this case following band limits in

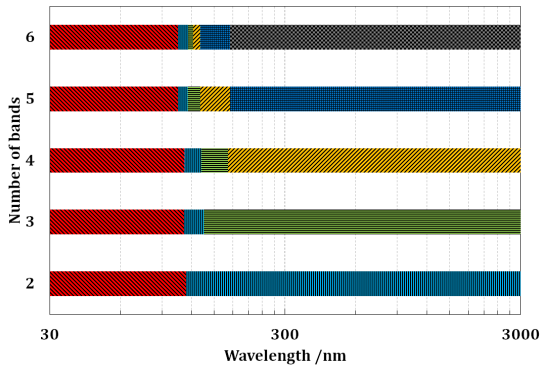

Figure 3. Optimized band boundaries of mean absorption coefficients for a 90% CO_2 – 10% C_4F_7N *gas mixture and diffuse temperature profile at 1 atm.*

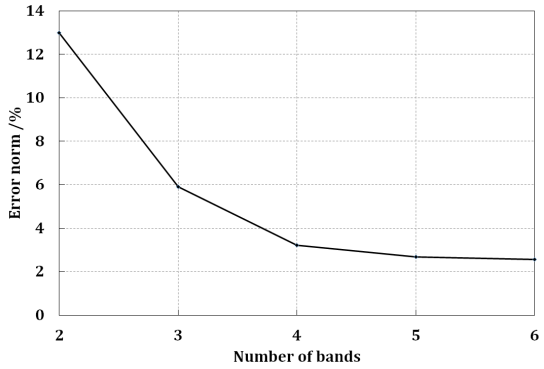

Figure 4. Error norm for a 90% CO_2 – 10% C_4F_7N *gas mixture and diffuse temperature profile at 1 atm.*

terms of wavelength are considered: the first band covers $\lambda = 30\,\text{nm}$ to $\lambda = 111.6849\,\text{nm}$, the second band covers $\lambda = 111.6849\,\text{nm}$ to $\lambda = 135.7897\,\text{nm}$, and the third band covers $\lambda = 135.7897\,\text{nm}$ to $\lambda = 29864.21\,\text{nm}$.

The divergence of the radiative flux along the domain radius as result of the spectrally resolved model is shown in Fig. 5 for the 90% CO_2 – 10% C_4F_7N gas mixture as well as for pure C_4F_7N, CO_2, SF_6, and air. The divergence of the radiative flux in the arc core for pure CO_2 is 6.9% larger compared to pure C_4F_7N . The 90% CO_2 – 10% C_4F_7N mixture shows the same profile of the divergence of the radiative flux in the arc core compared to pure CO_2 due to small mass fraction of C_4F_7N in the gas mixture. Small differences between profiles are observed only in the reabsorption region. Compared to pure SF_6, the cooling term is increased by almost 100 % for pure C_4F_7N.

3. CFD simulations

The commercial finite-volume solver *ANSYS® Fluent* [8] is used to model free burning SF_6, air, and 90% CO_2 – 10% C_4F_7N arcs that are stabilized by natural convection. The governing equations consist of the compressible hydrodynamic equations including the $k-\varepsilon$ turbulence model and the simplified set of Maxwell equations [9]. The discrete ordinate

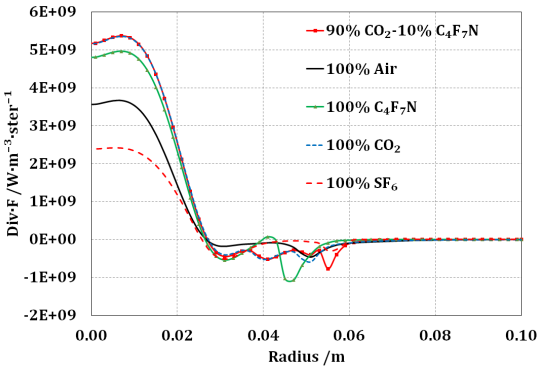

Figure 5. Divergence of radiative flux for various gas mixtures, spectral resolved model.

method (DOM) in *ANSYS® Fluent* is used to solve the radiation transport in the plasma using Planck mean absorption coefficients as presented in above section. The plasma is treated as a single-fluid at local thermodynamic equilibrium (LTE) and the necessary thermodynamic and transport properties of the pure gases and gas mixtures are calculated according to [9].

A 2D axi-symmetric geometry was defined to model free burning arcs as investigated in [10]. The simulation domain has a radius of $R = 1.5\,\text{cm}$ (y-direction, see Fig. 6), the distance between the electrodes is $d = 1.5\,\text{cm}$ (x-direction, see Fig. 6), and the distance between gas inlet (max. x-coordinate, see Fig. 6) and outlet (min. x-coordinate, see Fig. 6) is $l = 2\,\text{cm}$. A constant current of 10 A is applied on vertical surfaces of electrodes (y-direction, see Fig. 6). The effect of gravitation is considered by means of a -1.34 Pa gauge pressure boundary condition at the outlet (gravity is acting in x-direction, see Fig. 6).

The resulting stationary arc temperature distributions for SF_6, air, and $C_4F_7N - CO_2$ arcs are shown in Fig. 6. Due to the pressure gradient between inlet and outlet, natural convection leads to a broadening of the plasma temperature profile close to outlet boundary condition. The calculated radial temperature profiles for SF_6, air, and $C_4F_7N - CO_2$ arcs at the midpoint between electrodes are given in Fig. 7. Additionally, radial temperature profiles from Lowke's paper are shown. The model results are in good agreement with Lowke's model results for SF_6 and air arcs in the central regions of the discharge. Slight deviation can be observed in the outer region of the plasma mainly because of different transport, thermodynamic, and radiation properties used in the models. It is well known that SF_6 is superior to air as an arc quenching medium, where the constricted radial temperature profile result in higher temperature gradients with larger heat conduction losses. This is one reason for a better performance of SF_6, besides a faster recovery compared to air due to its electronegativity.

The $C_4F_7N - CO_2$ arc has more constricted radial profile than the arc in air, but it is more diffuse in

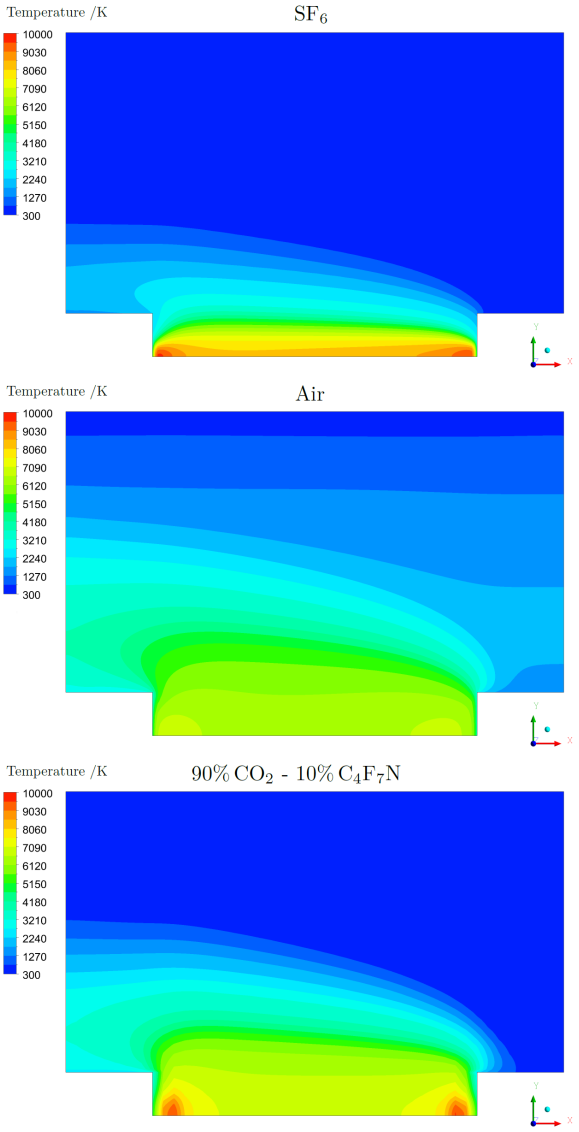

Figure 6. Temperature distribution of 10 A free burning arcs in various gases.

comparison to SF_6 arc. This is an indication for a weaker arc quenching performance of a $C_4F_7N - CO_2$ gas mixture compared to SF_6.

4. Conclusions

$C_4F_7N - CO_2$ gas mixtures are promising candidates to replace SF_6 in medium and high voltage switchgear applications. In this contribution, radiative properties of a specific $C_4F_7N - CO_2$ gas mixture have been calculated that can be utilized as input data for arc models of medium and high voltage switchgear. An optimization procedure was performed for a 90% CO_2 – 10% C_4F_7N gas mixture and defined temperature profiles to find the optimal number of spectral bands and spectral band interval limits. CFD simulations of free burning 90% CO_2 – 10% C_4F_7N arcs that are stabilized by natural convection, are carried out and compared with arcs burning in SF_6 and air. The calculated temperature profile of the arc in 90% CO_2 – 10% C_4F_7N gas mixture is more diffuse compared to the SF_6, which indicates a weaker arc extinguishing performance.

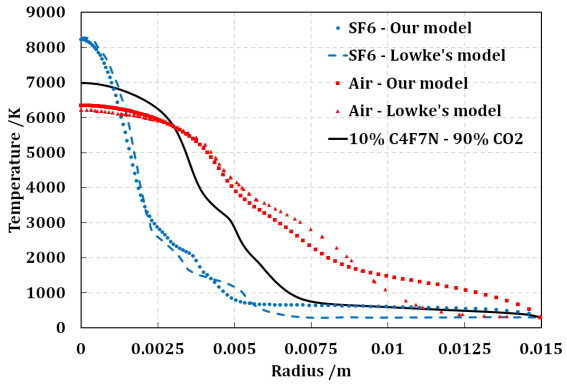

Figure 7. Calculated temperature profiles for the 10 A arcs at midpoint between electrodes.

Acknowledgements

The authors thank P. Kloc and M. Bartlova for providing the radiation database. This work is part of the project Nr. TH03020063 of the Technological Agency of the Czech Republic.

References

[1] V. Narayanan et al. Transport properties of thermal plasma containing fluoro-nitrile (C_4F_7N)-based gas mixtures. *Plasma Physics and Technology*, 6(2):131, 2019. doi:10.14311/ppt.2019.2.131.

[2] A. Gleizes et al. Thermal plasma modelling. *J Phys D: Appl Phys*, 38(9):R153, 2005. doi:10.1088/0022-3727/38/9/R01.

[3] M. F. Modest. *Radiative Heat Transfer*. Third edition. Academic Press, 2013.

[4] H. Nordborg and A. Iordanidis. Self-consistent radiation based modelling of electric arcs: I. efficient radiation approximations. *J Phys D: Appl Phys*, 41(13):135205, 2008. doi:10.1088/0022-3727/41/13/135205.

[5] P. Kloc, V. Aubrecht, and M. Bartlova. Numerically optimized band boundaries of Planck mean absorption coefficients in air plasma. *J Phys D: Appl Phys*, 50(30):305201, 2017. doi:10.1088/1361-6463/aa7627.

[6] P. Kloc et al. On the selection of integration intervals for the calculation of mean absorption coefficients. *Plasma Chem Plasma Process*, 35:1097–1110, 2015. doi:10.1007/s11090-015-9648-3.

[7] M. Gnybida, C. Rümpler, and V. Narayanan. Optimal band selection for the calculation of Planck mean absorption coefficients. *Plasma Physics and Technology*, 4(1):70, 2017. doi:10.14311/ppt.2017.1.70.

[8] ANSYS®. Release 17.1, ANSYS, Inc., 2016.

[9] C. Rümpler and V. Narayanan. Arc modeling challenges. *Plasma Physics and Technology*, 2(3):261–270, 2015.

[10] J. J. Lowke. Calculated properties of vertical arcs stabilized by natural convection. *J. Appl. Phys.*, 50(1):147, 1978. doi:10.1063/1.325698.